HHS Public Access

Author manuscript

J Bone Miner Res. Author manuscript; available in PMC 2016 July 01.

Published in final edited form as:

J Bone Miner Res. 2015 July ; 30(7): 1268–1279. doi:10.1002/jbmr.2458.

Single-Limb Irradiation Induces Local and Systemic Bone Loss in a Murine Model

Laura E. Wright, Ph.D.[1,¥], **Jeroen T. Buijs, Ph.D.**[1,¥], **Hun-Soo Kim, M.D.**[1], **Laura E. Coats, M.D.**[1], **Anne M. Scheidler, M.D.**[1], **Sutha K. John, M.S.**[1], **Yun She, B.A.**[1], **Sreemala Murthy, M.S.**[1], **Ning Ma, M.D.**[1], **Helen J. Chin-Sinex, B.S.**[2], **Teresita M. Bellido, Ph.D.**[3], **Ted A. Bateman, Ph.D.**[4], **Marc S. Mendonca, Ph.D.**[3], **Khalid S. Mohammad, M.D., Ph.D.**[1], and **Theresa A. Guise, M.D.**[1,*]

[1]Department of Medicine, Indiana University School of Medicine, Indianapolis, IN, USA

[2]Department of Radiation Oncology, Indiana University School of Medicine, Indianapolis, IN, USA

[3]Department of Anatomy and Cell Biology, Indiana University School of Medicine, Indianapolis, IN, USA

[4]Department of Biomedical Engineering and Radiation Oncology, University of North Carolina, Chapel Hill, NC, USA

Abstract

Increased fracture risk is commonly reported in cancer patients receiving radiotherapy, particularly at sites within the field of treatment. The direct and systemic effects of ionizing radiation on bone at a therapeutic dose are not well characterized in clinically relevant animal models. Using twenty-week male C57Bl/6 mice, effects of irradiation (right hindlimb; 2 Gy) on bone volume and microarchitecture were evaluated prospectively by microcomputed tomography and histomorphometry and compared to contralateral-shielded bone (left hindlimb) and non-irradiated control bone. One-week post-irradiation, trabecular bone volume declined in irradiated tibiae (−22%; $p<0.0001$) and femora (−14%; $p=0.0586$) and microarchitectural parameters were compromised. Trabecular bone volume declined in contralateral tibiae (−17%; $p=0.003$), and no loss was detected at the femur. Osteoclast number, apoptotic osteocyte number and marrow adiposity were increased in irradiated bone relative to contralateral and non-irradiated bone, while osteoblast number was unchanged. Despite no change in osteoblast number one-week post-irradiation, dynamic bone formation indices revealed a reduction in mineralized bone surface and a concomitant increase in unmineralized osteoid surface area in irradiated bone relative to contralateral and non-irradiated control bone. Further, dose- and time-dependent calvarial culture and *in vitro* assays confirmed that calvarial osteoblasts and osteoblast-like MC3T3 cells were relatively radioresistant, while calvarial osteocyte and osteocyte-like MLO-Y4 cell apoptosis was

[*]Address correspondence to: Theresa A. Guise, M.D., Indiana University, 980 West Walnut Street, Walther Hall R3, #C130, Indianapolis, IN 46202, Tele: 1.317.278.6014, Fax: 1.217.278.2912, tguise@iu.edu.

[¥]Authors contributed equally to this work.

Authors' roles: Study design: LEW, JTB, TMB, TAB, MSM, KSM, TAG. Study conduct and data collection LEW, JTB, HSK, LEC, AMS, SKJ, YS, SM, NM, HJC. Data analyses: LEW, JTB, HSK, LEC, AMS. Data interpretation: LEW, JTB, TMB, TAB, MSM, KSM, TAG. Drafting manuscript: LEW. Revising manuscript content and approving final version of the manuscript: All authors. LEW and JTB take responsibility for the integrity of the data analyses.

induced as early as 48h post-irradiation (4 Gy). In osteoclastogenesis assays, radiation exposure (8 Gy) stimulated murine macrophage RAW264.7 cell differentiation and co-culture of irradiated RAW264.7 cells with MLO-Y4 or murine bone marrow cells enhanced this effect. These studies highlight the multi-faceted nature of radiation-induced bone loss by demonstrating direct and systemic effects on bone and its many cell types using clinically relevant doses and have important implications for bone health in patients treated with radiation therapy.

Keywords

Radiation; Microarchitecture; Osteoclasts; Osteoblast; Osteocyte; Marrow adiposity

Introduction

Irradiation at sites of malignancy in adjunct with surgery and/or chemotherapy has proven to be an effective anti-cancer strategy that reduces mortality rates.[1] As disease-free survival continues to improve with effective treatment approaches, long-term side effects of radiotherapy on the skeletal system have emerged. A typical treatment regimen of ionizing radiation for gynecological cancers consists of administration of up to 60 Gy fractionated over a six-week span.[2,3] Healthy by-standing tissue, including bone, is estimated to absorb up to half of this dose (~30 Gy).[3,4] Despite efforts to minimize dose-limiting side effects by protecting healthy tissues, the incidence of pathological fracture at sites in the direct path of therapeutic irradiation is reportedly increased relative to non-irradiated skeletal sites in cancer patients and survivors.[5–11] Patients receiving radiotherapy for pelvic tumors including cervical, rectal and anal cancers have increased risk of hip fracture relative to cancer patients who undergo surgery or chemotherapy alone.[6–11] Likewise, a dose-dependent relationship between radiation and rib fracture incidence has been identified in breast cancer patients.[5] In addition to evidence for direct effects of radiation therapy on bone, systemic reduction in bone density has been detected in cancer patients within the first year of radiotherapy,[7,12,13] and radiation-treated breast cancer patients are reported to have hip fracture rates up to 20 times higher than average reported fracture rates for breast cancer patients four years after diagnosis.[14–16] Taken together, these striking clinical findings implicate that both direct and systemic mechanisms are at play in the pathology of radiation-induced bone loss.

While the deleterious effects of ionizing radiation on bone are widely accepted,[3,17] the direct and systemic mechanism(s) of radiation-induced bone loss at the cellular level are not well characterized, particularly in models which mimic a clinical setting of radiotherapy where exposure occurs at a localized site. Effects of radiation on bone typically have been characterized using total-body irradiation models where widespread systemic inflammation and radiation-induced hypogonadism can complicate data interpretation with regard to bone. Here we present results using a murine model of radiotherapy wherein the right hindlimb was selectively irradiated at a relatively low, clinically relevant dose of 2 Gy. Direct and indirect radiation-induced changes in bone volume and microarchitectural structures of bone were monitored prospectively for one week at irradiated bone sites and contralateral-shielded bone sites, and compared to sham-irradiated age-matched non-irradiated controls.

The skeletal response to irradiation is further characterized at the cellular level *in vivo* through quantitative histomorphometric analysis and *in vitro*.

Materials and Methods

Animals

The animal protocols utilized for these studies were approved by the Institutional Animal Care and Use Committee at Indiana University in accordance with the National Institutes of Health Guide for the Care and Use of Laboratory Animals. Twenty-week male C57Bl/6 mice were purchased from Harlan Laboratories (Indianapolis, IN) and housed in plastic cages with access to water and mouse chow *ad libitum* and maintained on a 12h light/dark schedule at 22±2°C. After one week of acclimation, mice were anesthetized with a ketamine/xylazine cocktail and underwent irradiation at a dose of 2 Gy (1.6 Gy/min for 1.25min; 320kV Precision X-ray machine) of a 2cm by 2cm area covering the right hindlimb, which included the femur, tibia and foot, while the contralateral limbs, torso (including reproductive organs) and head were covered with a malleable lead shield. Control mice were similarly manipulated, anesthetized, and underwent sham irradiation (0 Gy).

Bone micro-computed tomography (μCT) imaging

Bone μCT was performed at the proximal metaphysis of the tibia and the distal metaphysis and mid-diaphysis of the femur using a high-resolution imaging system (μCT40; Scanco Medical AG) on isoflurane-anesthetized mice. MicroCT scans were acquired using a $10\mu m^3$ isotropic voxel size, 55kVp peak X-ray tube potential, 200ms integration time, and were subjected to Gaussian filtration. Trabecular bone microarchitecture was evaluated in the proximal metaphysis of the tibia in a region that began 0.4mm distal to the growth plate and extended distally 1.0mm, and at the femoral distal metaphysis in a region that began 0.5mm proximal to the growth plate and extended proximally 1.0mm. A threshold of 170mg HA/cm^3 was used to segment bone from surrounding soft tissue. Trabecular bone outcomes included trabecular bone volume fraction (BV/TV; %), trabecular thickness (Tb.th; mm), trabecular number (Tb.N; mm^{-1}), trabecular separation (Tb.Sp; mm), and connectivity density (Conn.D; mm^{-3}). We chose to examine both the distal femur and proximal tibia bone sites in order to gain a more complete picture of the effects of single-site irradiation on bone. Scan acquisition and analyses were conducted in accordance with guidelines for use of μCT in rodents.[18]

Dual-energy X-ray absorptiometry (DXA) imaging

In vivo measurement of fat mass, lean mass and bone mineral density (BMD) was performed on anesthetized mice (ketamine/xylazine) using a PIXImus II densitometer (GE Lunar, Madison, WI) calibrated with a phantom of defined density. Total body composition and BMD of the proximal tibia and distal femur were analyzed at baseline one day prior to irradiation and at the termination of the study one week post-irradiation in order to assess a percent change over time.

Bone histology and histomorphometry

Hindlimbs were removed from mice at the time of experimental termination, fixed in 10% neutral-buffered formalin for 48h and stored in 70% ethanol. Tibiae were decalcified in 10% EDTA for two weeks, processed using an automated tissue processor (Excelsior, Thermoelectric), and embedded in paraffin. Mid-sagittal 3.5μm sections were stained with hematoxylin and eosin (H&E) with orange G and phloxine to visualize new bone, and with TRAP stain (tartrate-resistant acid phosphatase) to visualize osteoclasts. The number of osteoclasts (N.Oc/BS) and osteoblasts (N.Ob/BS) were identified and quantitated relative to the bone surface, and the total number of adipocytes distal to the growth plate in the proximal tibial metaphysis were quantified and expressed as adipocytes/mm^2. Paraffin embedded sections were evaluated for apoptotic nuclei by detection of terminal deoxynucleotidyl transferase dUTP nick end labeling (TUNEL), as per manufacturer's protocol (Klenow FragEL™ Fragmentation Detection Kit; Calbiochem).

In order to assess dynamic bone parameters, undecalcified femora were dehydrated in graded alcohol (70–100%), cleared in xylene, and infiltrated and embedded with methyl methacrylate (MMA) under vacuum. Using an automated microtome (Microm HM 360, Thermo Scientific), 45μm transverse sections were removed from the femoral diaphysis at the midsection and mounted unstained on standard microscope slides. Bones were double-labeled with calcein at the day of irradiation and at day six prior to the scheduled terminal necropsy at day seven to measure the following dynamic parameters: bone formation rate/bone surface (BFR/BS; $\mu m^3/\mu m^2$/day), mineral apposition rate (MAR; μm/day) and mineralizing surface (MS/BS; %). In order to differentiate mineralized and osteoid bone tissue, sections were deplasticized, rehydrated, stained with von Kossa and counterstained with tetrachrome (MacNeal; Polysciences) for improved contrast. Non-mineralized osteoid bone tissue was assessed by measurement of the following parameters: osteoid volume (OV/BS), osteoid surface (OS/BS) and osteoid width (μm). All sections were viewed on a Leica DM LB compound microscope outfitted with a Q-Imaging Micropublisher Cooled CCD color digital camera (Nuhsbaum Inc, McHenry, IL). Images were captured and analyzed using BioQuant Image Analysis Software version 12.1 (BIOQUANT Image Analysis Cooperation, Nashville, TN).

Calvarial bone culture assays

Calvariae were excised under sterile conditions from four-day-old Swiss White mice, cut in mid-sagitally, and incubated in 1mL of BGJ medium (Sigma) with 1% BSA, as previously described.[19] Calvarial bone cultures were irradiated on the same day of excision (0.244 Gy/min; Faxitron X-ray; n=4/group) or treated with insulin as a positive control for bone formation (100μg/mL) and cultured up to ten days with media refreshment occurring every 72h. Bones were fixed, decalcified, paraffin-embedded, and sectioned. The total number of osteoblasts and new bone area (%) were quantified in blinded fashion on H&E stained sections, as previously described,[19] and apoptotic (TUNEL+) osteoblasts and osteocytes were quantitated and expressed as a percentage of the total for each respective cell type.

Flow cytometry

Murine calvarium-derived preosteoblastic MC3T3 cells (ATCC) and murine long bone-derived osteocyte-like MLO-Y4 cells[20] were cultured in alpha-MEM with L-glutamin supplemented with antibiotics. Cells were seeded in 12-well plates (100,000 cells/well), grown to 80% confluence over a 48h period and irradiated with 2–20 Gy using 160kVp X-ray at a dose rate of 2.44 Gy/min (Faxitron Bioptics, LLC Tucson, AZ) or treated with dexamethasone (Sigma) as a positive control for apoptosis. Washed and trypsinized cells were resuspended in 500μL of binding buffer containing 5μL of Annexin V-EGFP and 5μL of propidium iodide (PI; Biovision). Tubes were incubated at room temperature for 5m in the dark. Annexin-V-EGFP binding and PI staining were assessed by flow cytometry using a FACSCalibur flow cytometer (BD Biosciences) and data were analyzed using Cell Quest software (BD Biosciences). The percentage of apoptotic cells was based on the evaluation of 10,000 events for each culture condition.

Osteoclastogenesis assays

Murine macrophage RAW264.7 cells (ATCC) were maintained in alpha-DMEM medium supplemented with antibiotics and 10% fetal bovine serum. Cells were seeded in 24-well plates (25,000/well) on a bone-mimetic surface (Corning OsteoSurface) in medium supplemented with deoxyribonucleosides, ribonucleosides, L-glutamine and RANKL (5–50ng/mL; R&D Systems) to stimulate osteoclastogenesis. In a parallel study, osteocyte-like MLO-Y4 or flushed bone marrow (BM) cells (125,000/well) were co-cultured with RAW264.7 cells under identical conditions. Briefly, BM cells were isolated under sterile conditions from the long bones of male C57Bl/6 mice and cultured on 90mm petri dishes for 2.5h at 37°C in alpha-DMEM and non-adherent BM cells were quantified and used for co-culture studies. Wells were irradiated with 160kVp X-rays at a dose rate of 2.44 Gy/min using 2 Gy fractions applied consecutively on days one to four over the course of one week, cumulating doses of 2–8 Gy for each treatment condition. Medium was refreshed on day 4 and cells were fixed on day seven and stained for TRAP activity. Osteoclasts, defined as TRAP+ multinucleated (≥3) cells, were quantified for each condition (n=4 wells/group). Cells were cleared from the plate surface with 10% bleach, washed, dried and resorption pits were visualized on a Leica DM LB compound microscope outfitted with a Q-Imaging Micropublisher Cooled CCD color digital camera (Vashaw Scientific Inc.). Images were captured and analyzed using MetaMorph software (Universal Imaging Corporation).

Statistical analyses

Differences were determined by one-way ANOVA, with Bonferroni post hoc testing, or by paired or unpaired student t test, as appropriate (GraphPad, Prism 6, version 6.0c). Results are expressed as mean ± SEM and $p<0.05$ was considered significant.

Results

Skeletal and body composition changes following localized irradiation of the right hindlimb

Local and systemic effects of single site exposure to ionizing radiation were assessed by measurement of trabecular bone volume and microarchitecture at the proximal tibia and distal femur. Use of μCT allowed us to delineate a purely trabecular region of interest such that changes in bone volume and microarchitectural structure in highly metabolically active trabecular compartments could be detected with precision.[18] Irradiated hindlimbs and contralateral lead-shielded hindlimbs were compared to hindlimbs from age-matched non-irradiated control mice. Seven days post-irradiation (2 Gy), trabecular bone volume (BV/TV; %), was reduced by 22% at the tibia and by 14% at the femur relative to baseline measurements in irradiated limbs (Fig. 1A–C; Table 1). These changes in irradiated bone were significant relative to changes observed in non-irradiated control tibiae and femora ($p<0.0001$ and $p<0.05$, respectively) (Fig. 1A–C). Bone volume of contralateral tibiae in irradiated mice was reduced by 17% relative to baseline measurements seven days post-irradiation (Fig. 1A,C; Table 1), and this decline was significant relative to changes in non-irradiated control bone volume at the tibia ($p<0.001$) (Fig. 1A,C). Further, bone microarchitecture was altered in irradiated bone, evidenced by a 50% reduction in connectivity density, a 16% reduction in trabecular number and a 20% increase in trabecular spacing relative to baseline measurements at the proximal tibia (Fig. 1D–F; Table 1). This loss of connectivity density was significant ($p<0.05$) relative to changes observed in sham control tibiae (Fig. 1D). At the femur, connectivity density and trabecular number were reduced by 45% and 13%, respectively, and spacing was increased by 16% relative to baseline measurements (Fig 1D–F; Table 1), with changes in trabecular number significantly reduced ($p<0.01$) relative to changes observed in sham control femora (Fig. 1E). Similar trends were detected at the microarchitectural level at contralateral bone sites (Fig 1D–G; Table 1); however, statistical significance was reached relative to changes observed in sham controls only in the case of reduced trabecular thickness ($p<0.05$) (Fig. 1G). Cortical bone properties at the femoral midshaft assessed by μCT were not different between groups (data not shown).

One week after irradiation of the right hindlimb, body weight declined significantly ($p<0.001$) relative to non-irradiated sham control mice (Fig. 2A). No change was observed in lean mass percentage between groups (Fig. 2B), as assessed by DXA, however, body fat mass declined significantly in irradiated animals one week after exposure (−22%; $p<0.0001$) (Fig. 2C), and this change could explain the observed decline in body weight. Changes in BMD by DXA, a 2-dimensional integration of bone that includes both trabecular and cortical bone compartments, were not detected at the proximal tibia or distal femur (Fig. 2D).

Cellular responses in bone to single site irradiation in vivo

Direct and systemic effects of focal irradiation *in vivo* were studied at the cellular level in bone tissue collected from irradiated and control mice. Quantitative histomorphometric analysis of TRAP+ osteoclasts revealed a statistically significant increase ($p<0.05$) in

osteoclast number in irradiated bone relative to contralateral and control tibiae one week after irradiation (Fig. 3A,B). No difference in osteoblast number was noted (Fig. 3C). Detection of fragmented DNA (TUNEL+) in osteocytes, an early stage marker of cellular apoptosis,[21] was increased in the trabecular bone compartment of irradiated bone compared to non-irradiated controls ($p<0.05$) (Fig. 3D). Quantitation of empty lacunae in trabecular bone, a late indicator of osteocyte death, revealed no significant differences between irradiated and non-irradiated bones in either trabecular or cortical bone compartments (Fig. 3E).

Dynamic histomorphometric analyses were carried out in order to determine whether osteoblast activity was altered one week post-irradiation. Bone formation rate (BFR/BS; $\mu m^3/\mu m^2/d$) was reduced ($p<0.05$) in irradiated femora relative to controls (Fig. 4B), and the mineralized surface relative to total bone surface (MS/BS) was likewise reduced in irradiated bone relative to both control ($p<0.01$) and contralateral femora ($p<0.05$) (Fig. 4D). Osteoblast activity was also assessed by measurement of its cellular byproduct, osteoid, or unmineralized bone matrix. Interestingly, we found that osteoid volume (OV/BV) and osteoid surface (OS/BS) were increased ($p<0.05$) in irradiated femora (Fig. 4E,F) relative to controls, and that the mean osteoid width was thicker ($p<0.05$) in bone that had been irradiated, relative to contralateral bone (Fig. 4G).

In alignment with previous reports of increased marrow adiposity following radiation therapy,[22] the adipocyte content of the marrow cavity of irradiated long bones was dramatically increased one week following exposure to 2 Gy ($p<0.001$) (Fig. 5A,B), and this effect was restricted to irradiated bones, with no differences detected in contralateral limbs relative to sham-control bone (Fig. 5A,B).

Differential response to irradiation by bone cells ex vivo

Next, we characterized the time- and dose-dependent effects of radiation on bone *in vitro* using a mouse calvarial bone formation assay. Consistent with results obtained from our *in vivo* studies, calvarial osteoblast number was not altered at any time point (1–10d) when irradiated at a dose of 2 Gy (Fig. 6A). Recapitulating our findings *in vivo*, though at a slightly later time point (10d vs. 7d), irradiation of bone at 2 Gy induced a significant increase in new bone ($p<0.01$) in irradiated calvarial tissue relative to non-irradiated control tissues (Fig. 6B). Exposure of bone to the higher dose of 10 Gy led to an eventual reduction in osteoblast number ($p<0.001$) relative to control tissues at the 10d time point, with no change in new bone formation at any time point (Fig. 6AB). Detection of TUNEL+ apoptotic osteoblasts in the same calvarial assay was negligible for all groups (Fig. 6C), however, similar to what was observed *in vivo*, osteocyte apoptosis was induced both dose- and time-dependently *in vitro* (Fig. 6D,E).

To further expand our understanding of the relative radiosensitivity of osteoblasts and osteocytes, we quantitated expression of Annexin V, a late stage marker of cellular apoptosis[23] using osteoblast-like MC3T3 cells and osteocyte-like MLO-Y4 cells. MC3T3 cell expression of Annexin V was significantly elevated at a dose of 10 Gy or higher 24h and 48h after radiation exposure ($p<0.05$ and $p<0.001$, respectively) (Fig. 7A,B). Very similar results were observed in MLO-Y4 cell populations (Fig. 7C), however, the dose-

response study at 48h post-irradiation revealed elevated expression of Annexin V ($p<0.05$) in osteocyte-like cells after as little as 4 Gy, and expression of Annexin V increased concomitantly with increasing doses of radiation up to 20 Gy (Fig. 7D,E).

Finally, effects of irradiation on osteoclastogenesis were evaluated using the murine macrophage osteoclast precursor cell line RAW264.7. Under minimal stimulation with the osteoclastogenic peptide RANKL (5ng/mL), direct irradiation of osteoclast precursor cells lead to a significant increase ($p<0.01$) in osteoclast number (Fig. 8A) and activity (Fig. 8B), as assessed by measurement of resorption pit area on a bone-mimetic surface, relative to non-irradiated control wells. These effects, however, were observed only at a cumulative dose of 8 Gy. Interestingly, irradiation at 8 Gy of a co-cultured population of RAW264.7 with osteocyte-like MLO-Y4 cells or with flushed murine bone marrow (BM) cells increased osteoclast differentiation by nearly six fold relative to the osteoclast numbers in wells with irradiated RAW264.7 cells alone ($p<0.05$) (Fig. 8A). Resorption area was increased in wells with an irradiated co-culture of RAW264.7 cells and BM cells relative to irradiated RAW264.7 cells alone (Fig. 8B), but no relative difference was observed in resorption pit area in irradiated wells of RAW264.7 cells combined with MLO-Y4 cells.

Discussion

Radiation-induced bone loss has historically been attributed to a long-term impairment of bone formation resulting from reduced osteoblast cell proliferation and the depletion of the adult stem cell population from which bone-forming osteoblast cells are derived.[7,13,24–26] Our results are in agreement with recent studies that challenge the view that radiation-induced bone loss is primarily a late-stage event,[16,27–29] as we present evidence for loss in trabecular bone volume and microstructure as early as one week post-irradiation. Furthermore, bone loss was detected in our model at sites of irradiation as well as at sites outside of the field of radiation, demonstrating that both local and systemic effects of irradiation have deleterious effects on the skeleton.

A rapid increase in osteoclastogenesis has been previously reported three days after total-body exposure.[28,29] Consistent with these reports, osteoclast number remained increased in trabecular bone one-week post-irradiation in our single-limb model. Interestingly, *in vitro* osteoclastogenesis assays presented here suggest that the direct effect of irradiation on osteoclast precursor cell differentiation is modest, but that irradiation of a co-culture of osteocyte-like cells or bone marrow cells with osteoclast precursors enhances osteoclastogenesis. These results indicate that signals from the osteocyte and/or bone marrow stroma may contribute to radiation-induced osteoclastic bone resorption. Using conditioned media collected from irradiated cells, we have yet to find evidence that soluble factors secreted from the osteocyte or bone marrow stroma are responsible for stimulation of osteoclastogenesis in this setting. Further studies will be required to identify possible signals within the bone microenvironment that contribute to osteoclast activation in the context of irradiation. The suppression of osteoclast activity using a bisphosphonate has previously been shown to abrogate radiation-induced bone loss in a preclinical model of total-body irradiation.[29] Collectively, preclinical data implicate a rapid and potentially sustained increase in osteoclastic bone resorption as one of the primary mechanisms of radiation-

induced bone loss, supporting the use of adjuvant anti-resorptive therapy for cancer patients undergoing radiotherapy.

In addition to an upregulation of osteoclastic bone resorption *in vivo*, dynamic bone indices revealed a defect in the formation of mineralized bone at sites of direct irradiation, supporting the long-standing notion that ionizing radiation impairs bone formation.[7,13,24–26,29] The timing however of these adverse effects on bone mineralization may occur sooner than previously thought, and moreover, impaired mineralization in our model was not driven by ablation of the osteoblast. To this point, the number of osteoblasts was not altered by 2 Gy exposure *in vivo*, consistent with our calvarial bone culture assays, which demonstrated that the proliferation of osteoblast cells was impaired only at higher doses (10 Gy) with no evidence of induction of apoptosis. Our *in vivo* and *in vitro* results consistently demonstrated that osteoblasts are relatively resistant to radiation-induced apoptosis. This is in full agreement with previous reports, which similarly demonstrate that osteoblast cells remain viable following exposure to doses between 10–30 Gy.[30,31] Despite the impaired mineralization, a compensatory surge in osteoblast apposition of new osteoid was detected in our studies one-week post-irradiation, and this effect occurred concomitantly with the sustained increase in osteoclastogenesis, suggesting that radiation exposure at this dose did not compromise the coupling of resorption and formation mediated by bone's basic multicellular unit.

Little is known about the role of the osteocyte in radiation-induced bone loss, and the few studies that do account for osteocyte-related outcomes report mixed results.[3,7,25,32] In our *in vivo* and *in vitro* models, doses of radiation as low as 2–4 Gy induced osteocyte apoptosis, providing evidence that the osteocyte may be highly sensitive to radiation exposure. Moreover, osteocytes appeared more radiosensitive than osteoblasts when compared head-to-head in proliferation and apoptosis assays. Impaired osteocyte function and/or cell death following radiation exposure could blunt the mechanosensitivity of bone and its response to dynamic loads, slowing bone growth and retarding bone repair, thus compromising its material strength. Radiation-induced osteocyte apoptosis may be a previously unappreciated contributor to the etiology of long-term bone loss and increased risk of fracture in cancer patients.

A reciprocal relationship has been identified clinically between marrow adiposity and bone volume in cancer patients treated with radiotherapy.[6,7,33] Consistent with these clinical findings, we report a near threefold increase in marrow adiposity in conjunction with >20% reduction in bone volume in irradiated tibiae. Radiation-induced DNA damage to bone marrow mesenchymal stem cells (MSCs) from which bone-forming osteoblasts are derived has been linked to cellular senescence resulting in reduced osteogenic potential and increased adipogenic potential of MSCs.[22,30,33–38] Despite no observed change in osteoblast number after one week, exhaustion of the MSC pool via an adipogenic lineage commitment switch could lead to a decrease in osteoblast number in our model at later time points, a postulate to be examined in future studies. While the underlying mechanisms responsible for fatty infiltration of the marrow following radiation exposure are still being clarified, it is clear that this marrow defect is strongly associated with bone loss and

increased fracture risk,[6,7,33] and that damage to MSCs following radiotherapy could drive this defect in human cancer patients.

Many groups have reported weight loss in mice following total-body irradiation due to systemic toxicity and bone marrow suppression.[39–41] The mechanism of body weight decline and loss in fat mass following focal hindlimb irradiation, as observed in our study, is not known. Significant reduction in body weight in men [42] and women[43] has been associated with reduced bone mineral density (BMD) and increased fracture risk over time in clinical trials. Systemic changes in body weight and body composition in our mice could be a contributing factor to bone loss bilaterally at both contralateral and irradiated bone sites.

The single-limb irradiation model utilized here is advantageous in that direct and systemic effects of radiation on bone can be delineated. In agreement with clinical reports of systemic osteopenia in radiation-treated cancer patients,[7,12,13] significant bone loss was detected at sites outside the field of irradiation in our mice. These results lend credence to the clinical-applicability of our model. Vascular damage, inflammation and the generation of reactive oxygen species (ROS) are thought to contribute to deleterious effects of radiation at distant skeletal and non-skeletal sites.[16,44] Histomorphometric differences at contralateral bone sites relative to control bone sites did not reach significance at one-week post-irradiation. Cellular changes in bone in the contralateral limbs (e.g., increased osteoclast numbers) likely occurred at an earlier time point following irradiation (<7 days post-irradiation), and thus, our data at the one-week time point did not capture these relatively acute changes at contralateral sites. Pro-resorptive inflammatory cytokines including interleukin (IL)-1, IL-6, IL-17 and tumor necrosis factor (TNF)-α are known to be highly elevated within 24–48hrs following radiation exposure,[44] likely driving early bone loss following irradiation.[28,29] Serum levels of IL-1, IL-6, IL-17 and TNF-α were assayed in our irradiated mice one-week post-irradiation, however, no differences were detected at this time point relative to control mice (data not shown), indicating that the period of increased inflammatory tone had likely subsided. Nevertheless, our finding of systemic bone loss following hindlimb radiation demonstrates that radiation-induced skeletal complications cannot be solely attributed to direct effects on bone, and the identification of the molecular mediator(s) of systemic bone loss could be important in developing bone-protective therapeutics for cancer patients.

While the prevention of pathological fractures in cancer patients is critical, other skeletal complications of radiation-induced bone loss may be important to consider. Multiple preclinical models have demonstrated that a heightened state of osteoclastic bone resorption can fuel the progression of cancer growth in bone.[45–47] Radiation-induced bone loss therefore could have serious implications with regard to cancer recurrence and skeletal metastasis in patients. During a state of heightened resorption, the bone microenvironment is rendered particularly favorable for cancer cell survival through the release of immobilized growth factors stored in the bone matrix (e.g., transforming growth factor-β, insulin-like growth factors, fibroblast growth factors, platelet-derived growth factor).[48–49] Additionally, osteoclast-derived proteolytic enzymes such as cathepsin-K and matrix metalloproteinase-9 have been shown to promote angiogenesis, cancer cell invasiveness and engraftment at metastatic sites.[47,49] Thus, it is critically important to monitor the skeletal health of cancer patients undergoing radiation treatment, or any anti-cancer therapeutic

known to adversely affect bone (e.g., glucocorticoids, anti-estrogen therapy, GnRH agonists), as treatment-induced bone loss could increase the likelihood of cancer recurrence in bone.[50] Adjuvant treatment with an anti-resorptive therapy may be considered in an effort to prevent treatment-induced skeletal complications. Preclinical studies will be necessary to determine whether radiation-induced bone loss (direct or systemic) can influence the progression of cancer bone metastases.

In summary, the etiology of radiation-induced skeletal complications appears multifactorial. In our therapeutic model of single-limb irradiation, osteoclast activation, osteocyte apoptosis and increased marrow adiposity, which is associated with MSC senescence, appear to contribute to bone loss at sites of direct irradiation. Similar to what is reported clinically, systemic bone loss was detected in our model at distant sites, indicating that local perturbations to the bone microenvironment can have wide-sweeping systemic effects. The identification of mediators and mechanisms of both direct and systemic radiation-induced bone loss could be important for the development of therapies that prevent skeletally related events in cancer patients and survivors. Further studies will be necessary to assess the full time course of changes in bone at the microarchitectural and cellular levels, at both irradiated and non-irradiated bone sites. Taken together, these studies expand our current understanding of the radiosensitivity of bone tissue to the insult of ionizing radiation and emphasize the multi-dimensional and often complex nature of bone loss.

Acknowledgments

Grant support: This work was supported by the Department of Defense Prostate Cancer Research Program postdoctoral training award PC101890 (LEW, JTB, HSK), the National Heart, Lung, and Blood Institute (NHLB/NIH) T35 HL110854 (LEC, AMS), the Jerry and Peggy Throgmartin Endowment (TAG), the Indiana Economic Development Fund, the National Cancer Institute (NCI/NIH) R01-CA69158 & U01-CA143057 (TAG), the V-Foundation (TAG), The Susan G. Komen Foundation (TAG), the National Institute of Arthritis and Musculoskeletal and Skin Diseases (NIAMS/NIH) R01-AR059221 (TAG) and a generous donation from the Withycombe Family (TAG).

References

1. Bernier J, Hall EJ, Giaccia A. Radiation oncology: a century of achievements. Nat Rev Cancer. 2004; 4:737–47. [PubMed: 15343280]
2. Meirow D, Nugent D. The effects of radiotherapy and chemotherapy on female reproduction. Hum Reprod Update. 2001; 7(6):535–43. [PubMed: 11727861]
3. Willey JS, Lloyd SAJ, Nelson GA, Bateman TA. Ionizing radiation and bone loss: space exploration and clinical therapy applications. Clin Rev Bone Miner Metab. 2011; 9(1):54–62. [PubMed: 22826690]
4. Sparks RB, Crowe EA, Wong FC, Toohey RE, Siegel JA. Radiation dose distribution in normal tissue adjacent to tumors containing ^{131}I or ^{90}Y: the potential for toxicity. J Nuclear Med. 2002; 43(8):1110–4.
5. Pierce SM, Recht A, Lingos TI, Abner A, Vicini F, Silver B, Herzog A, Harris JR. Long-term radiation complications following conservative surgery (CS) and radiation therapy (RT) in patients with early stage breast cancer. Int J Radiat Oncol Biol Phys. 1992; 23:912–923.
6. Baxter NN, Habermann EB, Tepper JE, Durham SB, Virnig BA. Risk of pelvic fractures in older women following pelvic irradiation. JAMA. 2005; 294(20):2587–93. [PubMed: 16304072]
7. Mitchell JM, Logan PH. Radiation-induced changes in bone. Radiographics. 1998; 18(5):1125–36. [PubMed: 9747611]

8. Williams HJ, Davies AM. The effect of X-rays on bone: a pictorial review. Eur Radiol. 2006; 16(3): 619–33. [PubMed: 16237551]

9. Kwon JW, Huh SJ, Yoon YC, Choi SH, Jung JY, Oh D, et al. Pelvic bone complications after radiation therapy of uterine cervical cancer: evaluation with MRI. AJR Am J Roentgenol. 2008; 191:987–94. [PubMed: 18806132]

10. Igdem S, Alco G, Ercan T, Barlan M, Ganiyusufoglu K, Unalan B, et al. Insufficiency fractures after pelvic radiotherapy in patients with prostate cancer. Int J Radiat Oncol Bio Phys. 2010; 77:818–23. [PubMed: 19879066]

11. Ikushima H, Osaki K, Furutani S, Yamashita K, Kishida Y, Kudoh T, et al. Pelvic bone complications following radiation therapy of gynecological malignancies: clinical evaluation of radiation-induced pelvic insufficiency fractures. Gynecol Oncol. 2006; 103:1100–4. [PubMed: 16919711]

12. Nishiyama K, Inaba F, Higashihara T, Kitatani K, Kozuka T. Radiation osteoporosis—an assessment using single energy quantitative computed tomography. Eur Radiol. 1992; 2(4):322–5.

13. Hopewell JW. Radiation-therapy effects on bone density. Med Pediatr Oncol. 2003; 41(3):208–11. [PubMed: 12868120]

14. Kirstensen B, Ejlertsen B, Mouridsen HT, Andersen KW, Lauritzen JB. Femoral fractures in postmenopausal breast cancer patients treated with adjuvant tamoxifen. Breast Cancer Res Treat. 1996; 39:321–6. [PubMed: 8877012]

15. Chen A, Maraicic M, Aragaki AK, Mouton C, Arendell L, Lopez AM, et al. Fracture risk increases after diagnosis of breast or other cancers in postemenopausal women: results from the Women's Health Initiative. Osteoporos Int. 2009; 20:527–36. [PubMed: 18766294]

16. Jia D, Gaddy D, Suva LJ, Corry PM. Rapid loss of bone mass and strength in mice after abdominal irradiation. Radiat Res. 2011; 176(5):624–35. [PubMed: 21859327]

17. Suva LJ, Griffin RJ. The irradiation of bone: old idea, new insight. J Bone Miner Res. 2012; 27(4): 747–8. [PubMed: 22434644]

18. Bouxsein ML, Boyd SK, Christiansen BA, Guldberg RE, Jepsen KJ, Muller R. Guidelines for assessment of bone microstructure in rodents using micro-computed tomography. J Bone Miner Res. 2010; 25(7):1468–86. [PubMed: 20533309]

19. Mohammad KS, Chirgwin JM, Guise TA. Assesssing new bone formation in neonatal calvarial organ cultures. Methods Mol Biol. 2008; 455:37–50. [PubMed: 18463809]

20. Kato Y, Windle JJ, Koop BA, Mundy GR, Bonewald LF. Establishment of an osteocyte-like cell line, MLO-Y4. J Bone Miner Res. 1997; 12(12):2014–23. [PubMed: 9421234]

21. Fawthrop DJ, Boobis AR, Davies DS. Mechanisms of cell death. Arch Toxicol. 1991; 65:437–44. [PubMed: 1929863]

22. Georgiou KR, Hui SK, Xian CJ. Regulatory pathways associated with bone loss and bone marrow adiposity by aging, chemotherapy, glucocorticoid therapy and radiotherapy. Am J Stem Cell. 2012; 1(3):205–24.

23. Vermes I, Haanen C, Steffens-Nakken H, Reutelingersperger CP. A novel assay for apoptosis. Flow cytometric detection of phosphatidylserine expression on early apoptotic cells using fluorescein labeled Annexin V. J Immunol Methods. 1995; 184:39–51. [PubMed: 7622868]

24. Sams A. The effect of 2000 r of x-rays on the internal structure of the mouse tibia. Int J Radiat Biol Relat Stud Phys Chem Med. 1966; 11(1):51–68. [PubMed: 4957987]

25. Ergun H, Howland WJ. Postradiation atrophy of mature bone. CRC Crit Rev Diagn Imagin. 1980; 12(3):225–43.

26. Green DE, Adler BJ, Chan ME, Rubin CT. Devastation of adult stem cell pools by irradiation precedes collapse of trabecular bone quality and quantity. J Bone Miner Res. 2012; 27(4):749–59. [PubMed: 22190044]

27. Kondo H, Searby ND, Mojarrab R, Phillips J, Alwood J, Yumoto K, Almeida EA, Limoli CL, Globus RK. Total-body irradiation of postpubertal mice with (137)Cs acutely compromises the microarchitecture of cancellous bone and increases osteoclasts. Radiat Res. 2009; 171(3):283–9. [PubMed: 19267555]

28. Willey JS, Lloyd SA, Robbins ME, Bourland JD, Smith-Sielicki H, Bowman LC, Norrdin RW, Bateman TA. Early increase in osteoclast number in mice after whole-body irradiation with 2 Gy X rays. Radiat Res. 2008; 170(3):388–92. [PubMed: 18763868]
29. Willey JS, Livingston EW, Robbins ME, Bourlard JD, Tirado-Lee L, Smith-Sielicki H, Bateman TA. Risedronate prevents early radiation-induced osteoporosis in mice at multiple skeletal locations. Bone. 2010; 46(1):101–11. [PubMed: 19747571]
30. Despars G, Caronneau CL, Bardeau P, Coutu DL, Beausejour CM. Loss of the osteogenic differentiation potential during senescence is limited to bone progenitor cell and is dependent on p53. PLOS ONE. 2013; 8(8):1–11.
31. Szymczyk KH, Shapiro IM, Adams CS. Ionizing radiation sensitizes bone cells to apoptosis. Bone. 2004; 34:148–56. [PubMed: 14751572]
32. Rabelo GD, Beletti ME, Dechichi P. Histological analysis of the alterations on cortical bone channels network after radiotherapy: a rabbit study. Microsc Res Tech. 2010; 73(11):1015–8. [PubMed: 20169617]
33. Hui SK, Khalil A, Zhang Y, Coghill K, Le C, Dusenbery K, Froelich J, Yee D, Downs L. Longitudinal assessment of bone loss from diagnostic computer tomography scans in gynecologic cancer patients treated with chemotherapy and radiation. Am J Obstet Gynecol. 2010; 203:353–57. [PubMed: 20684943]
34. Cao X, Wu Z, Frassica D, Yu B, Pang L, Xian L, Wan M, Lei W, Armour M, Tryggestad E, Wong J, Wen CY, Lu WW, Frassica FJ. Irradiation induces bone injury by damaging bone marrow microenvironment for stem cells. Proc Natl Acad Sci USA. 2011; 108(4):1609–14. [PubMed: 21220327]
35. Carbonneau CL, Despars G, Rojas-Sutterlin S, Fortin A, Le O, et al. Ionizing radiation-induced expression of INK4a/ARF in murine bone marrow-derived stromal cell populations interferes with bone marrow homeostasis. Blood. 2012; 119:717–26. [PubMed: 22101896]
36. Qui J, Zhu G, Chen X, Shao C, Gu S. Combined effects of gamma-irradiation and cadmium exposures on osteoblasts in vitro. Environ Toxicol Pharmacol. 2012; 33:149–57. [PubMed: 22209727]
37. Komori T. Regulation of bone development and maintenance by Runx2. Front Biosci. 2008; 13:898–903. [PubMed: 17981598]
38. Su W, Chen Y, Zeng W, Liu W, Sun H. Involvement of Wnt signaling in the injury of murine mesenchymal stem cells exposed to X-radiation. Int J Rad Biol. 2012; 88(9):635–41. [PubMed: 22724383]
39. Nunamaker EA, Artwohl JE, Anderson RJ, Fortman JD. Endpoint refinement for total body irradiation of C57Bl/6 mice. Comp Med. 2013; 63(1):22–8. [PubMed: 23561934]
40. Duran-Struuck R, Dysko RC. Principles of bone marrow transplantation (BMT): providing optimal veterinary and husbandry care to irradiated mice in BMT studies. J Am Assoc Lab Anim Sci. 2009; 48(1):11–22. [PubMed: 19245745]
41. Xun CQ, Thompson JS, Jennings CD, Brown SA, Widmer MB. Effect of total body irradiation, busulfan-cyclophosphamide, or cyclophosphamide conditioning on inflammatory cytokine release and development of acute and chronic graft-versus-host disease in H-2-incompatible transplanded SCID mice. Blood. 1994; 83(8):2360–7. [PubMed: 8161803]
42. Meyer HE, Sogaard AJ, Falch JA, Jorgensen L, Emaus N. Weight change over three decades and the risk of osteoporosis in men: The Norwegian Epidemiological Osteoporosis Studies (NOREPOS). Am J Epidemiol. 2008; 168(4):454–60. [PubMed: 18599490]
43. Ensrud KE, Ewing SK, Stone KL, Cauley JA, Bowman PJ, Cummings SR. Intentional and unintentional weight loss increase bone loss and hip fracture risk in older women. J Am Geriatr Soc. 2003; 51(12):1740–7. [PubMed: 14687352]
44. Lorimore SA, Coates PJ, Scobie GE, Miline G, Wright EG. Inflammation-type responses after exposure to ionizing radiation in vivo: a mechanism for radiation-induced bystander effects? Oncogene. 2001; 20(48):7085–95. [PubMed: 11704832]
45. Ottewell PD, Wang N, Brown HK, Reeves KJ, Fowles CA, Croucher PI, et al. Zoledronic acid has differential anti-tumor activity in pre- and post-menopausal bone microenvironment in vivo. Clin Cancer Res. 2014; 20:1–11.

46. Ottewell PD, Wang N, Meek J, Fowles AM, Croucher PI, Eaton CL, Holen I. Castration-induced bone loss triggers growth of disseminated prostate cancer cells in bone. Endocr Relat Cancer. 2014 Oct; 21(5):769–81. Epub 2014 Jul 22. [PubMed: 25052474]

47. Wright LE, Guise TA. The microenvironment matters: estrogen deficiency fuels cancer bone metastases. Clin Cancer Res. 2014; 20(11):2817–9. [PubMed: 24803577]

48. Mohan S, Baylink DJ. Bone growth factors. Clin Orthop Relat Res. 1991; 263:30–48. [PubMed: 1993386]

49. Weilbaecher KN, Guise TA. Cancer to bone: a fatal attraction. Nature Rev Cancer. 2011; 11:411–25. [PubMed: 21593787]

50. Ratajczak MZ, Jadczyk T, Schneider G, Kakar SS, Kucia M. Induction of a tumor-metastasis-receptive microenvironment as an unwanted and underestimated side effect of treatment by chemotherapy or radiotherapy. J Ovarian Res. 2013; 6:95. [PubMed: 24373588]

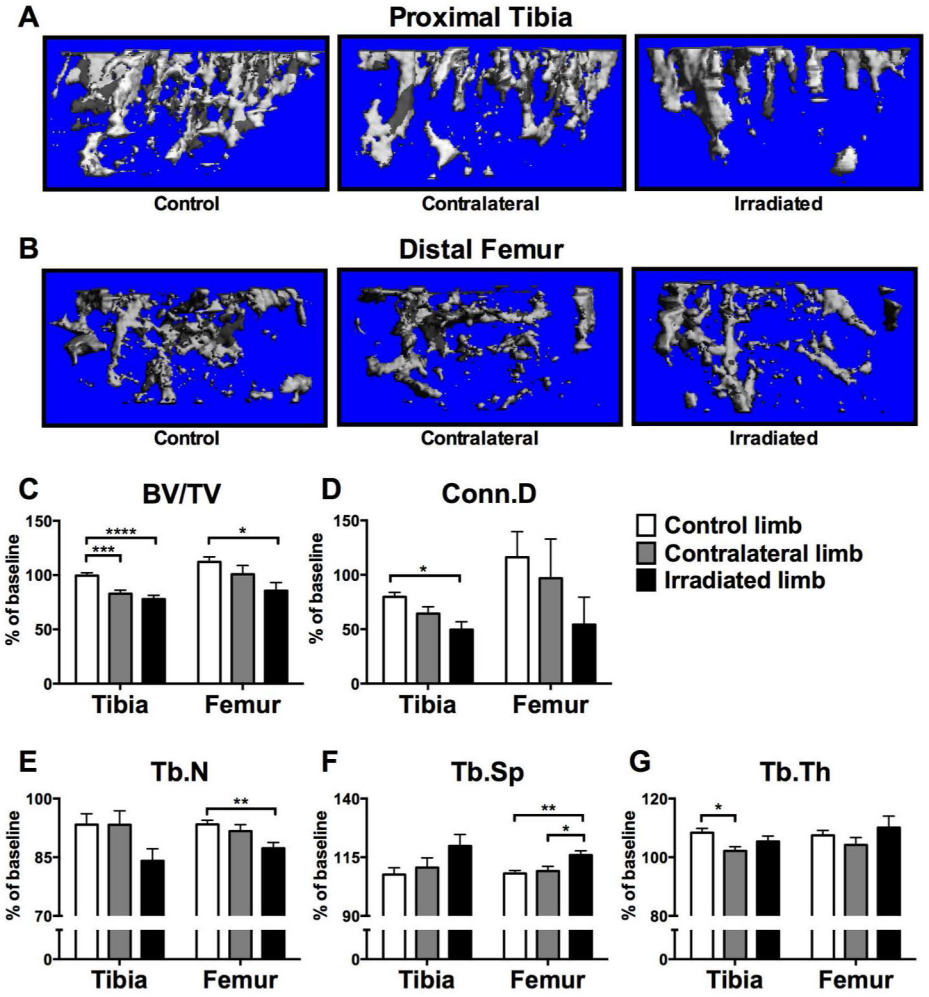

Figure 1.

Effects of *in vivo* radiation exposure (2 Gy) to the right hindlimb on bone volume and trabecular microarchitecture in irradiated and non-irradiated (contralateral) bone of twenty-week male C57Bl/6 mice one week post-irradiation relative to sham-irradiated control mice, as assessed by micro-computed tomography (μCT; SCANCO Viva40CT; 10μm voxel size, 55kVp, 200ms integration time). Representative reconstructed images of μCT scans showing trabecular bone at the (A) proximal tibia and (B) distal femur were selected with a BV/TV % most representative of the group mean. Differences in (C) bone volume fraction (BV/TV), (D) connectivity density (Conn.D), (E) trabecular number (Tb.N), (F) trabecular spacing (Tb.Sp) and (G) trabecular thickness (Tb.Th) are presented as mean ±SEM of change relative to baseline with differences determined by one-way ANOVA with post-hoc testing (*p<0.05, **p<0.01, ***p<0.001, ****p<0.0001; n=28 control, n=16 contralateral, n=16 irradiated).

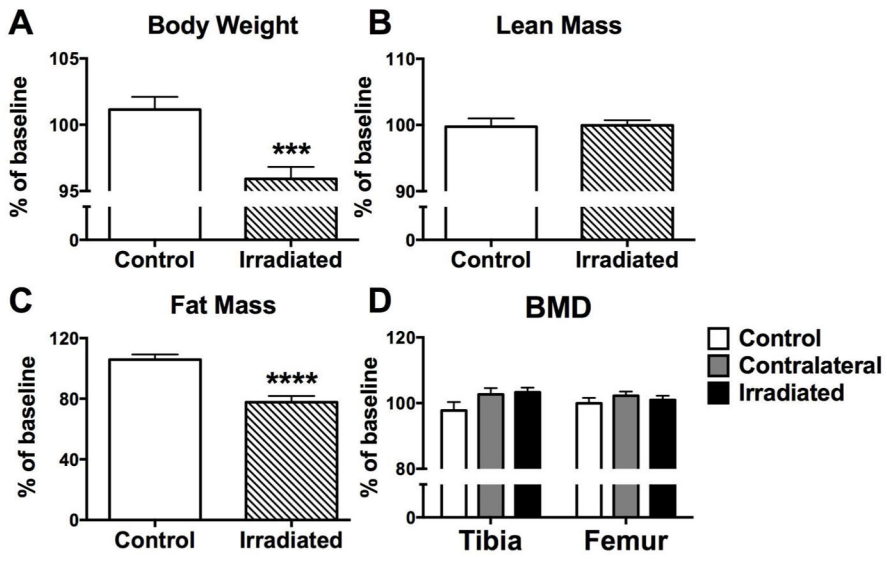

Figure 2.

Effects of *in vivo* radiation exposure (2 Gy) to the right hindlimb on (A) body weight, (B) total body lean mass, (C) total body fat mass and (D) bone mineral density (BMD) of the proximal tibia and distal femur in twenty-week male C57Bl/6 mice as assessed by dual energy X-ray absorptiometry (DXA). Data are expressed as mean percent change ±SEM relative to baseline measurements one week post-irradiation with differences determined by unpaired t test where ***$p<0.001$ and ****$p<0.0001$ (n=16/group).

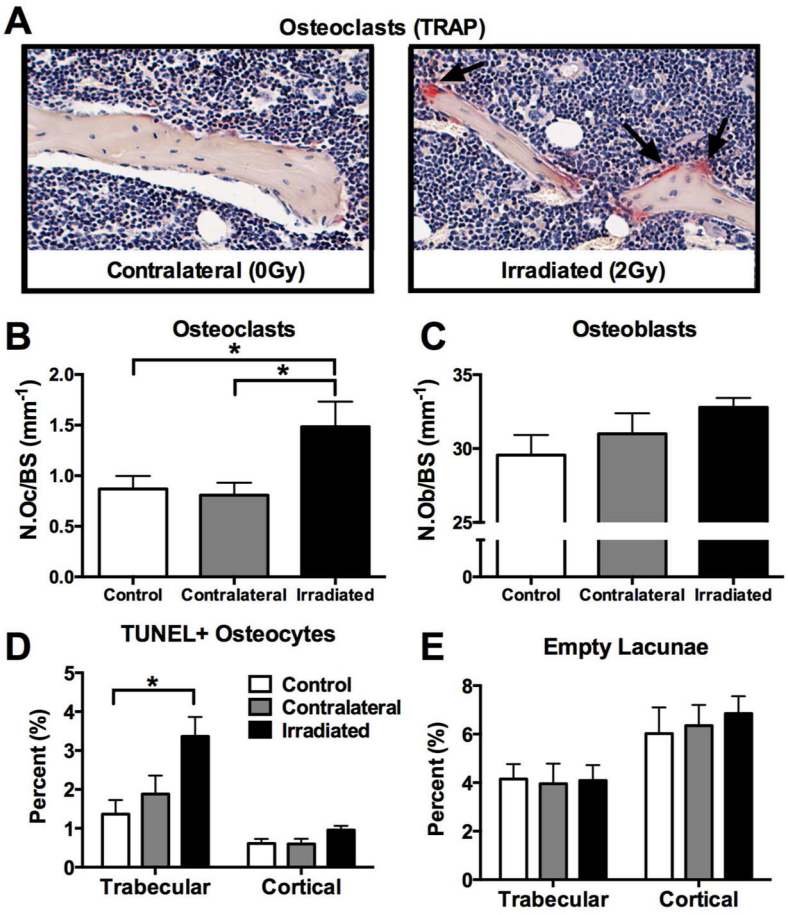

Figure 3.

Effects of *in vivo* radiation exposure (2 Gy) to the right hindlimb on (A,B) osteoclasts, (C) osteoblasts, (C) apoptotic (TUNEL+) osteocytes and (D) empty lacunae in irradiated and non-irradiated (contralateral) bone relative to sham-irradiated control bone one week post-irradiation. Results are presented as mean ±SEM with differences determined by one-way ANOVA with post-hoc testing where $p<0.05$.

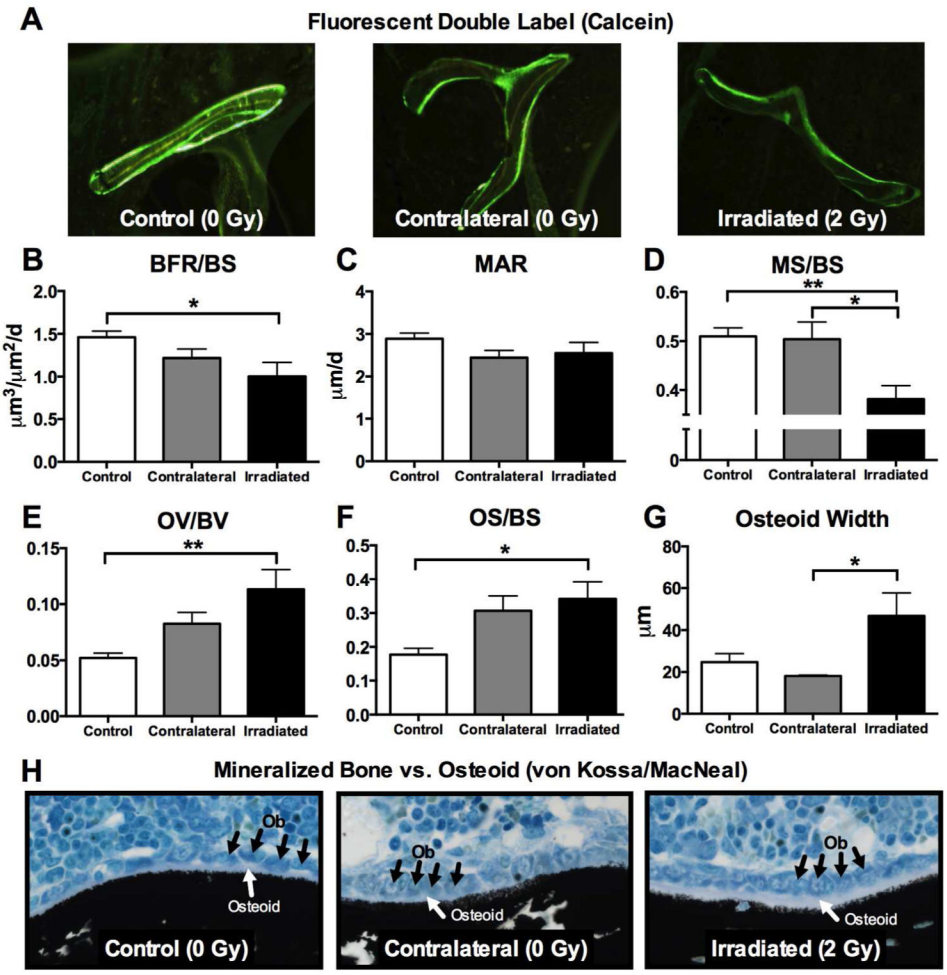

Figure 4.

Effects of *in vivo* radiation exposure (2 Gy) to the right hindlimb on (B) bone formation rate (BFR/BS) (C) mineral apposition rate (MAR) (D) mineralized bone surface (MS/BS), (E) osteoid volume (OV/BV), (F) osteoid surface (OS/BS) and (G) osteoid width in irradiated and non-irradiated (contralateral) bone relative to sham-irradiated control bone one week post-irradiation. (A) Representative calcein-labeled bone sections are presented. (H) Representative von Kossa/MacNeal-stained sections show osteoblasts (black arrows) and osteoid bone (white arrows) relative to mineralized bone (black stain). Results are presented as mean ±SEM with differences determined by one-way ANOVA with post-hoc testing where *p<0.05 and **p<0.01.

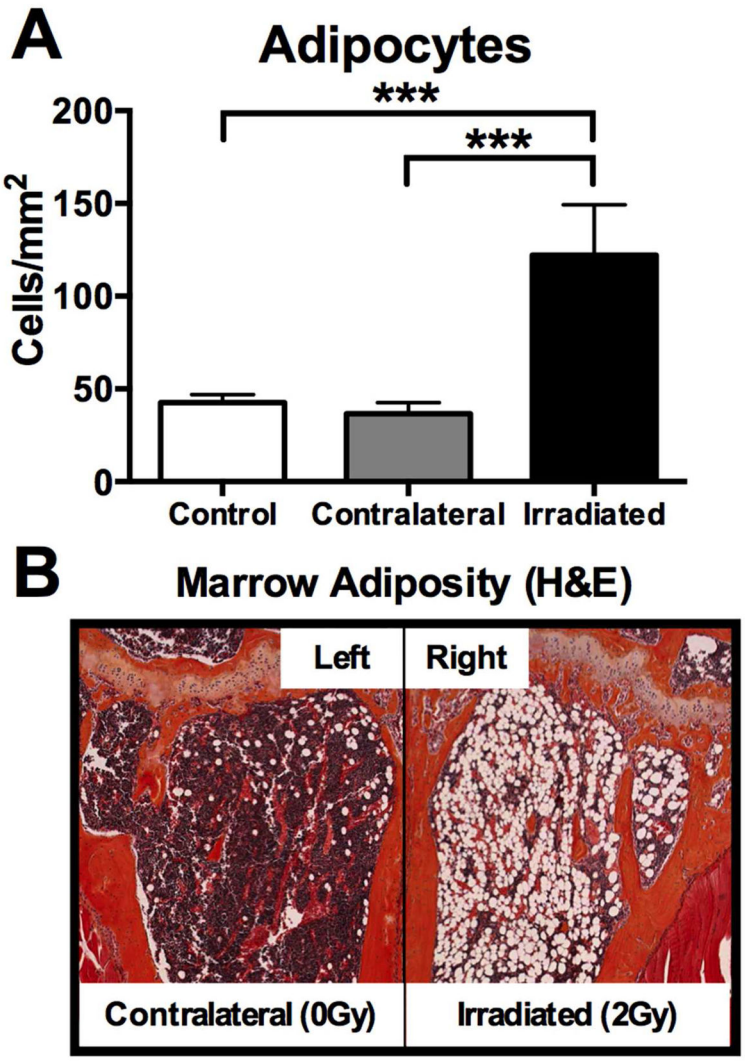

Figure 5.

Effects of *in vivo* radiation exposure (2 Gy) to the right hindlimb on marrow adiposity in irradiated (right) and non-irradiated contralateral (left) bone relative to sham-irradiated control bone one week post-irradiation. (A) Results are presented as mean ±SEM with differences determined by one-way ANOVA with post-hoc testing (***$p<0.001$). (B) H&E sections of the left (contralateral) and right (irradiated) proximal tibiae of the same animal are presented.

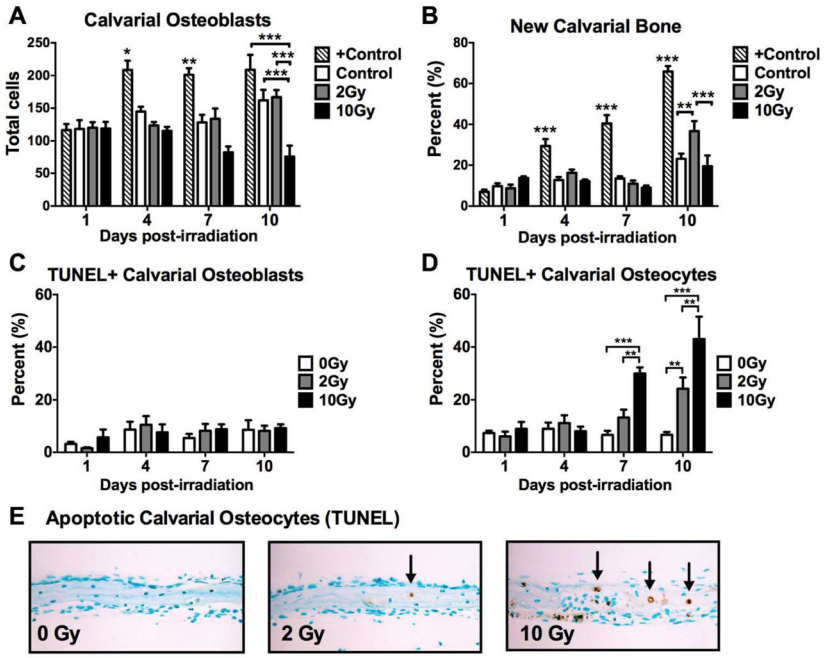

Figure 6.

Effects of *in vitro* irradiation of mouse calvarial tissue on (A) osteoblasts, (B) new bone formation, (C) apoptotic (TUNEL+) osteoblasts and (D) apoptotic osteocytes. (E) Representative histological sections show TUNEL+ osteocytes (black arrows). Results are presented as mean ±SEM with differences determined by one-way ANOVA with post-hoc testing where **p*<0.05, ***p*<0.01 and ****p*<0.001 (*n*=4/group) relative to 0 Gy.

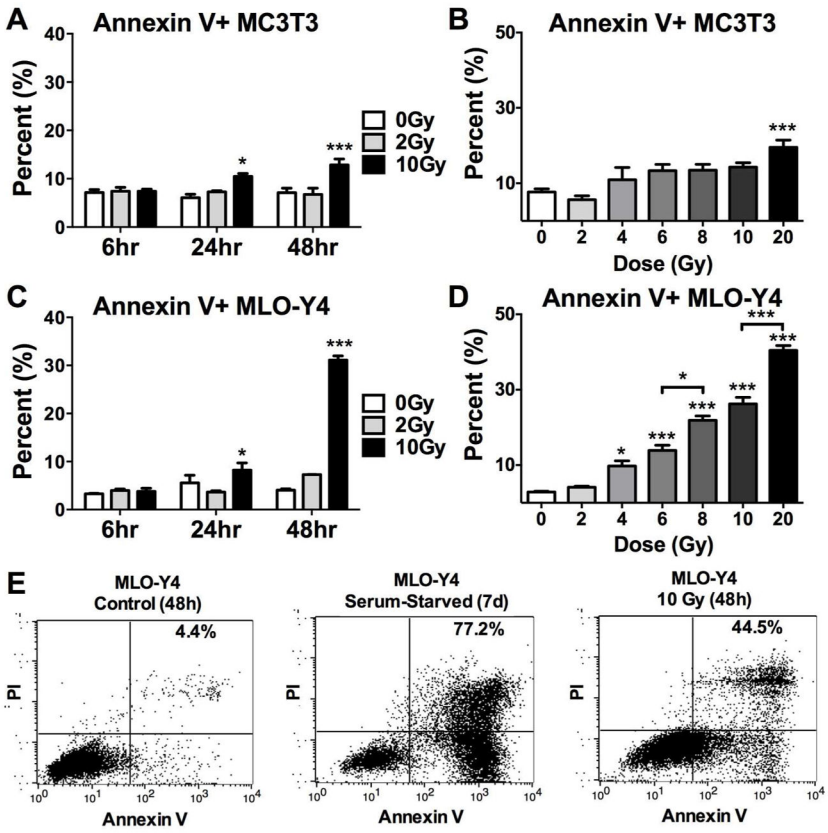

Figure 7.

Time and dose-dependent effects of irradiation on cellular apoptosis of (A,B) osteoblast-like MC3T3 cells and (C–E) osteocyte-like MLO-Y4 cells *in vitro*, as assessed by flow cytometry. Results are presented as mean ±SEM with differences determined by one-way ANOVA with post-hoc testing where **p*<0.05 and ****p*<0.001 relative to 0 Gy.

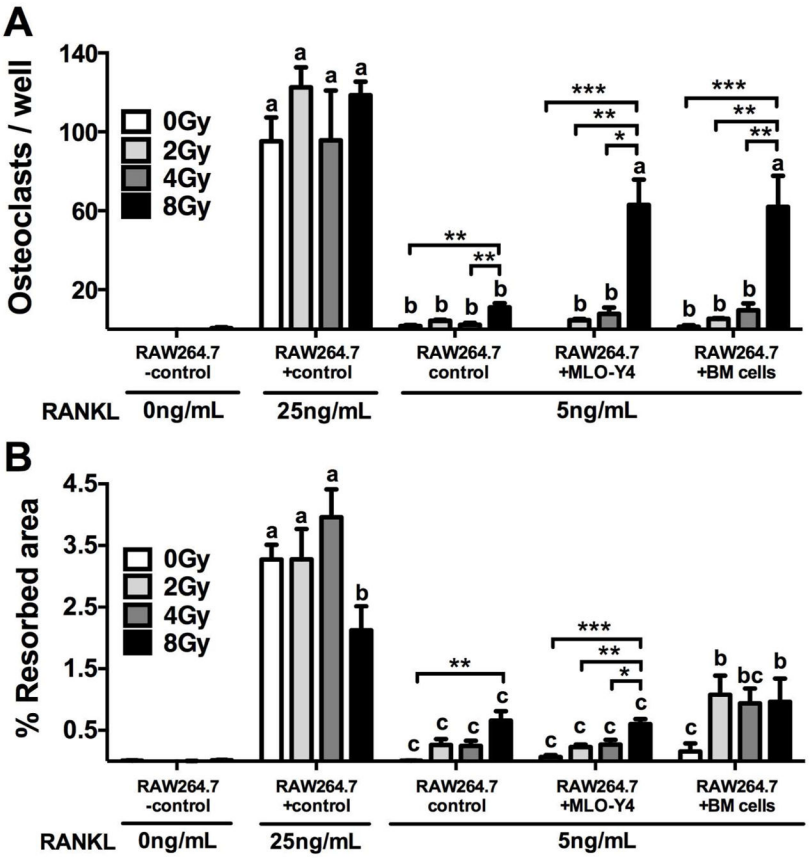

Figure 8.

Cumulative dose-dependent effects of radiation on (A) osteoclastogenesis and (B) resorption activity of RAW264.7 cells alone or in co-culture with MLO-Y4 cells or bone marrow (BM) cells. Results are presented as mean ±SEM with differences determined by one-way ANOVA with post-hoc testing where *$p<0.05$, **$p<0.01$ and ***$p<0.001$. Means without a common letter differ significantly as determined by one-way ANOVA of all treatment conditions with post-hoc testing where $p<0.05$.

Table 1

Outcomes for Trabecular Bone Microarchitecture

	BV/TV (%)			Conn.D (1/mm^3)			Tb.N (1/mm)			Tb.Th (mm)			Tb.Sp (mm)		
	Mean (SD)	**% change**	***P****	**Mean (SD)**	**% change**	***P****	**Mean (SD)**	**% change**	***P****	**Mean (SD)**	**% change**	***P****	**Mean (SD)**	**% change**	***P****
Proximal Tibia															
Control	7.05(0.98)	−0.45	0.8632	27.0 (7.6)	−20	**0.0001**	2.65 (0.38)	−6.7	**0.0209**	0.056 (0.004)	8.4	**<0.0001**	0.405 (0.07)	7.6	**0.0139**
Contralateral	5.95(0.01)	−17	**0.0003**	19.9 (5.0)	−36	**0.0002**	2.62 (0.40)	−6.7	0.0752	0.053 (0.004)	2.2	0.1701	0.407 (0.06)	11	**0.0192**
Irradiated	5.24(0.01)	−22	**<0.0001**	13.6 (6.5)	−50	**0.0002**	2.24 (0.29)	−16	**0.0003**	0.056 (0.005)	5.4	**0.0088**	0.473 (0.06)	20	**0.0005**
Distal Femur															
Control	4.49(0.012)	12	**0.0102**	14.8(0.32)	16	0.2595	2.90 (0.27)	−6.6	**<0.0001**	0.055 (0.005)	7.4	**0.0001**	0.356 (0.03)	8.1	**<0.0001**
Contralateral	3.49 (0.008)	0.8	0.9127	10.5 (5.6)	−3.1	0.9038	2.74 (0.27)	−8.3	**0.0001**	0.051 (0.006)	4.2	0.1153	0.375 (0.04)	9.1	**0.0005**
Irradiated	3.43 (0.009)	−14	0.0586	7.13 (4.6)	−46	**0.0005**	2.60 (0.34)	−13	**<0.0001**	0.058 (0.008)	10	**0.0316**	0.400 (0.05)	16	**<0.0001**

% change is expressed relative to baseline measurments prior to treatment.

* *P* value is obtained from paired t-test with baseline measurements where $n = 28$ for control, $n = 16$ for contralateral and $n = 16$ for irradiated bones.